

Experimental realization of the weak value of polarization anisotropy: a new concept of “weak value polarimeter”

Niladri Modak¹, Athira B S², Ankit Kumar Singh¹, Nirmalya Ghosh^{1,2,*}

¹*Department of Physical Sciences,*

Indian Institute of Science Education and Research (IISER) Kolkata.

Mohanpur 741246, India

²*Center of Excellence in Space Sciences India,*

Indian Institute of Science Education and Research (IISER) Kolkata.

Mohanpur 741246, India

*Corresponding author: ngghosh@iiserkol.ac.in

Abstract

Using the concept of weak measurements in classical optics, we introduce a new polarimetry tool that is capable of amplifying and quantifying extremely small sample polarization anisotropy effects, namely, linear and circular diattenuation and retardance. The approach is founded on interferometric realization of weak value of polarization observable and is experimentally obtained by *near* destructive interference of polarized light in a Mach-Zehnder interferometer in the presence of a *weak* polarization anisotropy effect. Real and imaginary weak value amplification of a given sample anisotropy effect manifests in different Stokes vector elements at the exit port of the interferometer, which follow orthogonal trajectories in the Poincare sphere. Remarkably, the *weak value polarimeter* enhances the sensitivity of quantification of a small sample anisotropy effect exactly by the large weak value amplification factor using traditional Stokes vector measurements. This opens up a new paradigm in the domain of polarimetry by extending the measurement limit far beyond conventional polarimeters.

Introduction

Optical polarimetry has played vital roles in understanding and developing various advanced concepts of electromagnetic waves [1], discovering a number of intricate and intriguing spin optical effects [2], uncovering molecular structure, organization and the nature of chemical bonds [3,4], quantifying chiral properties of proteins and other biological molecules [5,6], probing anisotropic organization and order of crystalline nanomaterials and other complex materials [7], developing polarization-based optical methods for biomedical imaging, remote sensing, meteorology, astronomy

and providing a variety of non-destructive evaluation methods [5,8-11]. Polarimetry techniques probe anisotropic polarizability of matter through the difference in refractive indices (RI) between orthogonal polarization states (for both linear and circular polarizations) that leads to the so-called birefringence (retardance) and dichroism (diattenuation) effects [9, 12-14]. Once accurately quantified, the polarization anisotropy parameters provide a wealth of interesting sample properties of potential importance. These polarization properties are traditionally quantified through multiple measurements of Stokes vector elements of sample-emerging light by cycling the input polarization state to selected polarizations [12, 13]. A more encompassing approach involves exhaustive measurement of the 4×4 Mueller matrix that contains complete information on the polarizing transfer function of any material medium [9, 14]. Despite their extensive use, these conventional polarimetry techniques are compromised when one needs to measure extremely small polarization effect, which is desirable for certain practical applications, e.g., for the detection of physiological glucose concentration in human tissue, for the quantification of extremely small circular dichroism of proteins, for the determination of weak magneto-optical rotation in nanomaterials and so on [9, 15]. Stokes vector or Mueller matrix measurements employing polarization modulation and synchronous detection schemes have been developed to overcome some of the related problems [9]. However, these measurement approaches are cumbersome and often require tedious calibration. Here, we introduce a simple non-modulation based novel polarimetry method based on the concept of optical weak measurement that is capable of quantifying extremely small sample polarization anisotropy effect going far beyond the limit of traditional polarimeters.

In recent times, weak measurements and weak value amplification (WVA) have proven to be useful in numerous optical experiments, in amplifying tiny spin optical effects, in high precision measurements of phase shift, frequency shift, temporal shift, ultra-small rotation, beam deflection etc. [16-24]. In these conventional pre-post selected optical weak measurements, Gaussian laser modes, temporal pulse, spectral line shapes etc. are used as pointer which are weakly coupled to the system through a weak optical effect that is to be amplified [16-25]. Polarization and angular momentum degrees of freedom of light are usually employed for obtaining mutually nearly orthogonal pre and post selection of states, which leads to WVA of tiny optical effect, manifesting as unusually large deflection of the pointer [26, 27]. Note that WVA phenomenon can be interpreted as near destructive interference between the *slightly* shifted pointer profiles as a result of mutually nearly orthogonal pre-post selections [27]. Using this simple yet profound philosophy of WVA, we present a new polarimetry tool, namely, *weak value polarimeter* that is capable of amplifying and quantifying extremely small sample polarization anisotropy effects. As opposed to conventional optical weak measurements [16-24], here, polarization state of light is used as pointer and small polarization anisotropy acts as the weak interaction. We experimentally demonstrate WVA of all the sample

polarization anisotropy effects (linear and circular diattenuation and retardance) by near destructive interference of a given input polarization state of light in one arm of an interferometer with *slightly* changed polarization state (due to the weak anisotropy effect) in the other arm. Real and imaginary WVA of a given anisotropy effect are manifested in different Stokes vector elements, which has fundamental quantum mechanical origin in the commutation relations of the Stokes polarization operators. On practical grounds, the novel ability of the weak value polarimeter to amplify and to dramatically enhance the sensitivity of quantification of extremely small sample polarization properties using simple traditional Stokes vector measurements is of general relevance to characterizing wide class of weakly anisotropic materials in diverse applications.

Theoretical framework of weak value polarimeter

The principle of the weak value polarimeter is based on realization of the weak value of a given polarization anisotropy effect through near destructive interference of polarized light in an interferometer in the presence of a *weak* polarization anisotropy effect. Near destructive interference in this scenario refers to destructive interference of two fields (having a phase difference π) with a small amplitude offset ($\epsilon_a = \tan^{-1} \frac{1-a}{1+a}$, a is the ratio of amplitudes of the two fields) between them or alternatively, interference of two fields having equal amplitude but with a phase difference of $(\pi \pm \epsilon_p, \epsilon_p$ is the small phase offset). The former generates a real WVA and the latter imaginary WVA. The $\epsilon_{a/p}$ parameters are equivalent to the small overlap of near orthogonal pre-post selected states in conventional weak measurements. In order to demonstrate WVA of all the polarization anisotropy effects (linear and circular diattenuation and retardance), we define the generalized polarization anisotropy parameter α in terms of the difference in RI (n) between orthogonal linear or circular polarizations as $2\alpha = \frac{2\pi}{\lambda} (n_{L/C}^{r/i} - n_{L'/C'}^{r/i}) t$. Here, t is the path length and the superscripts (r/i) correspond to real/imaginary parts of RI and the subscripts (L/C) and (L'/C') represent linear/circular polarizations and their orthogonal states, respectively. The real / imaginary parts of RI are associated with diattenuation /retardance effects [13].

WVA of diattenuation

Linear diattenuation

We consider interference of $+45^\circ$ polarized light in one path with slightly changed polarization state after experiencing a small linear diattenuation effect between horizontal (x) and vertical (y) polarization components in the other path. The corresponding electric field vectors are

$$\mathbf{E}_1 = \frac{\hat{x} + \hat{y}}{\sqrt{2}}; \mathbf{E}_2 = \frac{e^{\alpha} \hat{x} + e^{-\alpha} \hat{y}}{\sqrt{e^{2\alpha} + e^{-2\alpha}}}; \quad (1)$$

The *imaginary* WVA of small linear diattenuation effect can be obtained by near destructive interference (small phase offset ϵ_p from exact destructive interference) of \mathbf{E}_1 and \mathbf{E}_2 to yield the resultant field \mathbf{E} as

$$\mathbf{E} = (\cos \epsilon_p \pm i \sin \epsilon_p) \mathbf{E}_1 - (\cos \epsilon_p \mp i \sin \epsilon_p) \mathbf{E}_2 \quad (2)$$

Using the components of the electric fields of Eq. (2), the four Stokes vector intensity elements ($S = [I \ Q \ U \ V]^T$) can be determined. In the so-called weak coupling limit ($\alpha \rightarrow 0$) [26], the circular (elliptical) polarization descriptor 4th Stokes vector element $\left(\frac{V}{I}\right)$ can be shown to exhibit WVA with decreasing ϵ_p as

$$\frac{V}{I} \approx \mp \alpha \cot \epsilon_p \quad (3)$$

The corresponding expressions for *real* WVA can be obtained by destructive interference of E_1 and E_2 with small amplitude offset ϵ_a to yield the resultant field as

$$\mathbf{E} = (\cos \epsilon_p \pm \sin \epsilon_p) \mathbf{E}_1 - (\cos \epsilon_p \mp \sin \epsilon_p) \mathbf{E}_2 \quad (4)$$

The *real* WVA in this case manifests in the linear polarization descriptor Stokes vector element $\left(\frac{Q}{I}\right)$ (in the limit of small $\epsilon_a \rightarrow 0$) as

$$\frac{Q}{I} \approx \mp \alpha \cot \epsilon_a \quad (5)$$

Note that the upper bound of WVA in Eq. (3) and (5) are set by the fundamental limit of degree of polarization (≤ 1) which limits the minimum value of $\epsilon_{a/p} (\leq \alpha)$. A pictorial representation of the electric field vectors and the polarization ellipse illustrating real and imaginary WVA of linear diattenuation effect are shown in **Figure 1a**. The corresponding evolutions of the Stokes vector polarization states show interesting trajectories in the Poincare sphere with varying $\epsilon_{a/p}$ (**Fig. 1a**). As evident, for real WVA, the polarization state evolves along the geodesic trajectory connecting the states of the two paths of the interferometer (the input state and the state after experiencing the weak anisotropy effect). For imaginary WVA on the other hand, the corresponding trajectory lies in a plane that is perpendicular to it. This appears to be a general rule for all the polarization anisotropy effects, results of which are presented subsequently.

Circular diattenuation

The WVA of small circular diattenuation effect can be formulated using the same framework as above taking any linear polarization state as input. The corresponding expressions for the fields \mathbf{E}_1 and \mathbf{E}_2 for input horizontal (x) polarization are noted in **Table 1**. This leads to *imaginary* and *real* WVA (respectively) of circular diattenuation in the Stokes vector elements as

$$\frac{U}{I} \approx \alpha \cot \epsilon_p \quad (6a)$$

$$\frac{V}{I} \approx \alpha \cot \epsilon_a \quad (6b)$$

The corresponding trajectories of polarization states in the Poincare sphere for varying $\epsilon_{a/p}$ are shown in **Fig. 1b**.

Generalized WVA of diattenuation and retardance

The above framework for WVA can be generalized for linear and circular retardance properties as summarized in **Table 1**. This concept can be experimentally realized using a conventional Mach-Zehnder interferometer (**Figure 1c**). The choice of the input state depends upon the polarization anisotropy effect to be amplified (see Table 1), which can be applied in one arm of the interferometer.

Although the above formalism of weak value polarimeter is based on simple classical EM theory model of polarized light, it has intriguing *quantum* mechanical equivalence. As evident, the real and the imaginary WVA of a given polarization anisotropy effect are manifested in different Stokes Vector elements ($Q, U \vee V$). The different Stokes polarization parameters therefore act as conjugate variables and their corresponding *quantum* operators must satisfy commutation relations and the respective variances are accordingly restricted by uncertainty relations [28, 29].

Experimental realization of weak value polarimeter

Experimental methods

The 632.8 nm line of a He-Ne laser is passed through a rotatable polarizer P1 (GTH10M-A, Thorlabs, USA) to make it linearly polarized at a desired angle and is then used to seed the interferometric weak value polarimetry system (**Fig. 1c**). The small polarization anisotropy effect is introduced in one arm using standard polarization optical elements (listed in **Table 1**). The light beams in the two arms with slightly different polarization states are then made to interfere at the exit port and the resulting fringes are imaged into a CCD camera (Micro Publisher 3.3, Qimaging, 2048 × 1536 square pixels, pixel dimension 3.45 μm). The spatially resolved Stokes vector elements across the interference fringe are measured using a combination of quarter waveplate QWP (WPMQ05M-633, Thorlabs, USA) and a linear polarizer P2. For the quantification of the *imaginary* WVA of a given anisotropy effect, the intensities of light in the two arms are kept equal and the recorded spatial variation of the relevant Stokes vector element (Table 1) around the position of the intensity minima or the destructive interference point is used to generate its variation as a function of the small phase offset parameter ϵ_p . In order to quantify the *real* WVA on the other hand, the relative intensities (or amplitude ratio a) of light in the two arms are varied using a variable neutral density filter ND (NDL-25C-2, Thorlabs, USA). The variation of the relevant Stokes vector element corresponding to the spatial position of the destructive interference is then generated as a function of the small amplitude offset parameter ϵ_a (or a) by combining multiple measurements.

Results and discussions

First, we illustrate the concept of WVA through simulation of the interference experiment taking linear retardance as the representative small polarization anisotropy effect. **Figure 2** presents simulation results for the interference of $+45^\circ$ polarized Gaussian light beam in one arm of a Mach-Zehnder interferometer with the beam having a slightly changed polarization state in the other arm due to a small linear retardance ($\alpha = 0.017\text{rad}$) effect. The experimental parameters are comparable to our experimental system (Fig. 1c). The $\frac{Q}{I}$ Stokes polarization parameter exhibits prominent enhancement at close vicinity of the intensity minima of the fringe corresponding to destructive interference position (**Fig. 2a**). Accordingly, the $\frac{Q}{I}$ parameter is observed to vary as $(\propto \alpha \cot \epsilon_p)$ with the small phase offset parameter ϵ_p (**Fig. 2b**), as a manifestation of *imaginary* WVA of small linear retardance α (see Table 1). The corresponding *real* WVA of α is manifested in the $\frac{V}{I}$ Stokes parameter (**Fig. 2c** and **Fig. 2d**). The $\frac{V}{I}$ parameter increases rapidly with decreasing amplitude offset parameter ϵ_a (shown for three different ϵ_a in **Fig. 2c**) and scales as $(\propto \alpha \cot \epsilon_a)$ (**Fig. 2d**) implying *real* WVA of linear retardance α .

The corresponding experimental results for the imaginary and real WVA of small linear ($x - y$) diattenuation effect ($\alpha = 0.017$) are summarized in **Figure 3**. Note that the role of the Stokes parameters in the imaginary and the real WVA of linear diattenuation effect are reversed as compared to linear retardance effect. Accordingly, the experimentally measured $\frac{V}{I}$ polarization parameter is observed to vary rapidly around the spatial position of the intensity minima and approaches its maximum value near the destructive interference point (**Fig. 3b**). The variation of $\frac{V}{I}$ with the ϵ_p parameter (**Fig. 3c**) shows very good agreement with the corresponding *imaginary* WVA prediction of Eq. 3 ($\propto \alpha \cot \epsilon_p$). Similarly, the experimentally measured variation of the $\frac{Q}{I}$ Stokes parameter also scales as $(\propto \alpha \cot \epsilon_a)$ with varying ϵ_a parameter (**Fig. 3d**) as predicted by Eq. 5 for *real* WVA. However, the quantitative agreement with the theoretical prediction seems to be slightly less accurate for the real WVA as compared to the imaginary counterpart. This arises because while the imaginary WVA results (Fig. 3c) are extracted from a single spatial map $\frac{V}{I}$, the real WVA results (Fig. 3d) are derived from multiple measurements of $\frac{Q}{I}$ for varying intensity ratios at the two arms, making the latter more prone to experimental errors. Never-the-less, these results demonstrate faithful imaginary and real WVA of small linear diattenuation effect. **Figure 4** provides experimental demonstration of WVA of small circular diattenuation effect ($\alpha = 0.012$). As expected, imaginary WVA is manifested here as rapid increase of the $\frac{U}{I}$ Stokes parameter with decreasing phase offset ϵ_p (**Fig. 4a**) and shows

excellent agreement with the corresponding prediction ($\propto \alpha \cot \epsilon_p$, Eq. 6a). Real WVA of circular diattenuation (**Fig. 4b**) is manifested as ($\propto \alpha \cot \epsilon_a$) scaling of the $\frac{V}{I}$ Stokes parameter as predicted by Eq. 6b. Experiments were also performed for imaginary and real WVA of small optical rotation effect using the specifics of the input state and the polarization optical element noted in Table 1. The results confirmed faithful imaginary and real WVA of small optical rotation α , which were reflected in ($\propto \alpha \cot \epsilon_{p/a}$) scaling of the $\frac{V}{I}$ and $\frac{U}{Q}$ Stokes polarization parameters, respectively (not shown here) [30].

The results presented above provide conclusive demonstration of real and imaginary WVA of all the polarization anisotropy effects. Note that the experimental WVA curves and their weak value fit for a given anisotropy effect serves the purpose to calibrate for an arbitrary scaling factor (which is observed to vary between $\sim 0.9 - 2.0$) of our experimental weak value polarimeter. This enables accurate quantification of small polarization anisotropy effect α of an unknown sample from the measured real and imaginary WVA of the respective Stokes parameters with knowledge of the $\epsilon_{a/p}$ parameters in the interferometer. This was further validated by performing experimental measurements for varying α for all the effects. Note that in conventional polarimeters, the maximum achievable sensitivity of quantification of a polarization anisotropy parameter (magnitude α) is typically of the order or lower than the sensitivity of determination of individual Stokes vector or Mueller matrix elements [9, 14]. The most remarkable feature of this weak value polarimeter is that it can accurately quantify the magnitude α that is smaller by a large weak value amplification factor ($\cot \epsilon_{a/p} \sim \frac{1}{\epsilon_{a/p}}$, where $\epsilon_{a/p} \ll 1$) than the corresponding sensitivity of determination of the respective Stokes vector elements. This provides the weak value polarimeter the unprecedented ability to amplify and quantify extremely small sample polarization effect by performing simple non-modulation-based dc measurements of the Stokes vector elements, thereby extending the measurement limit far beyond conventional polarimeters.

Conclusions

We have introduced a new polarimetry concept, namely weak value polarimeter that uses interferometric realization of WVA of polarization observable to achieve unprecedented sensitivity in determination of extremely small sample polarization anisotropy effect. WVA of all the sample anisotropy effects are experimentally demonstrated using a Mach-Zehnder interferometric configuration. Real and imaginary WVA of a given sample anisotropy effect manifest themselves in different Stokes vector elements, which evolve in orthogonal trajectories in the Poincare sphere. This manifestation of WVA of polarization has an intriguing *quantum* mechanical equivalence in the

commutation relations of the Stokes polarization operators. From a practical point of view, the weak value polarimeter extends the measurement sensitivity of traditional polarimeters, which is of general relevance for the quantification of extremely small sample anisotropy properties of wide range of materials in diverse applications. Finally, the weak value polarimeter is breaking new ground in polarization measurements and its extension to the other established domains of polarimetry like in spectroscopic and imaging polarimetry remains to be explored. We are currently expanding our investigations in these directions by integrating interferometric spectroscopy and imaging and microscopy methods [31-33] in the framework of weak value polarimeter.

References:

1. K. Y. Bliokh, A. Niv, V. Kleiner, and E. Hasman, "Geometrodynamics of spinning light," *Nat. Photonics*2, 748 (2008).
2. K. Y. Bliokh, D. Smirnova, and F. Nori, "Quantum spin hall effect of light," *Science*348, 1448–1451 (2015).
3. M.-L. Ren, R. Agarwal, P. Nukala, W. Liu, and R. Agarwal, "Nanotwin detection and domain polarity determination via optical second harmonic generation polarimetry," *Nanoletters*16, 4404–4409 (2016).
4. T. Lowry, "Polarimetric methods in chemistry," (1934).
5. B. Jirgensons, *Optical activity of proteins and other macro-molecules*, vol. 5 (Springer Science & Business Media, 2012).
6. R. S. Gurjar, V. Backman, L. T. Perelman, I. Georgakoudi, K. Badizadegan, I. Itzkan, R. R. Dasari, and M. S. Feld, "Imaging human epithelial properties with polarized light scattering spectroscopy," *Nat. medicine*7, 1245–1248(2001).
7. M. J. Fasolka, L. S. Goldner, J. Hwang, A. Urbas, P. DeRege, T. Swager, and E. L. Thomas, "Measuring local optical properties: near-field polarimetry of photonic block copolymer morphology," *Phys. review letters*90, 016107 (2003).
8. M. Gadsden, P. Rothwell, and M. J. Taylor, "Detection of circularly polarised light from noctilucent clouds," *Nature*278, 628–629 (1979).
9. N. Ghosh and A. I. Vitkin, "Tissue polarimetry: concepts, challenges, applications, and outlook," *J. biomedical optics*16, 110801 (2011).
10. A. Chrysostomou, P. W. Lucas, and J. H. Hough, "Circular polarimetry reveals helical magnetic fields in the young stellar object hh 135–136," *Nature*450, 71–73 (2007).

11. D. Stam, J. Hovenier, and L. Waters, "Using polarimetry to detect and characterize jupiter-like extrasolar planets," *Astron. & Astrophys.*428, 663–672 (2004).
12. D. H. Goldstein, *Polarized light* (CRC press, 2016).
13. S. D. Gupta, N. Ghosh, and A. Banerjee, *Wave optics: Basic concepts and contemporary trends* (CRC Press, 2015).
14. R. Azzam, "Propagation of partially polarized light through anisotropic media with or without depolarization: a differential 4×4 matrix calculus," *JOSA.*68, 1756–1767(1978).
15. V. Belotelov, I. Akimov, M. Pohl, V. Kotov, S. Kasture, A. Vengurlekar, A. V. Gopal, D. Yakovlev, A. Zvezdin, and M. Bayer, "Enhanced magneto-optical effects in magneto-plasmonic crystals," *Nat. Nanotechnol.*6, 370 (2011).
16. N. Ritchie, J. G. Story, and R. G. Hulet, "Realization of a measurement of a "weak value"," *Phys. review letters*66,1107 (1991).
17. O. Hosten and P. Kwiat, "Observation of the spin hall effect of light via weak measurements," *Science*319, 787–790(2008).
18. A. K. Singh, S. K. Ray, S. Chandel, S. Pal, A. Gupta, P. Mitra, and N. Ghosh, "Tunable fano resonance using weak value amplification with asymmetric spectral response as a natural pointer," *Phys. Rev. A*97, 053801 (2018).
19. O. S. Magaña-Loaiza, M. Mirhosseini, B. Rodenburg, and R. W. Boyd, "Amplification of angular rotations using weak measurements," *Phys. Rev. Lett.*112, 200401 (2014).
20. P. B. Dixon, D. J. Starling, A. N. Jordan, and J. C. Howell, "Ultrasensitive beam deflection measurement via interferometric weak value amplification," *Phys. review letters*102,173601 (2009).
21. G. Puentes, N. Hermosa, and J. Torres, "Weak measurements with orbital-angular-momentum pointer states," *Phys. review letters*109, 040401 (2012).
22. S. Kocsis, B. Braverman, S. Ravets, M. J. Stevens, R. P. Mirin, L. K. Shalm, and A. M. Steinberg, "Observing the average trajectories of single photons in a two-slit interferometer," *Science*332, 1170–1173 (2011).
23. M. Asano, K. Bliokh, Y. Bliokh, A. Kofman, R. Ikuta, T. Ya-mamoto, Y. Kivshar, L. Yang, N. Imoto, S. Özdemir et al., "Anomalous time delays and quantum weak measurements in optical micro-resonators," *Nat. communications*7, 1–9(2016)
24. J. Z. Salvail, M. Agnew, A. S. Johnson, E. Bolduc, J. Leach, and R. W. Boyd, "Full characterization of polarization states of light via direct measurement," *Nat. Photonics*7, 316(2013).
25. J. Dressel, M. Malik, F. M. Miatto, A. N. Jordan, and R. W. Boyd, "Colloquium: Understanding quantum weak values: Basics and applications," *Rev. Mod. Phys.*86, 307 (2014).

26. Y. Aharonov, D. Z. Albert, and L. Vaidman, "How the result of a measurement of a component of the spin of a spin-1/2 particle can turn out to be 100," *Phys. review letters* 60, 1351 (1988).
27. I. Duck, P. M. Stevenson, and E. Sudarshan, "The sense in which a " weak measurement" of a spin-1/2 particle's spin component yields a value 100," *Phys. Rev. D* 40, 2112 (1989).
28. N. Korolkova, G. Leuchs, R. Loudon, T. C. Ralph, and C. Silberhorn, "Polarization squeezing and continuous-variable polarization entanglement," *Phys. Rev. A* 65, 052306 (2002).
29. W. P. Bowen, N. Treps, R. Schnabel, and P. K. Lam, "Experimental demonstration of continuous variable polarization entanglement," *Phys. review letters* 89, 253601 (2002).
30. S. Guchhait, N. Modak, J. K. Nayak, A. Panda, M. Pal, N. Ghosh et al., "Weak value amplification using spectral interference of fano resonance," *arXiv preprint arXiv:1903.10256* (2019).
31. F. Huth, M. Schnell, J. Wittborn, N. Ocelic, and R. Hillenbrand, "Infrared-spectroscopic nanoimaging with a thermal source," *Nat. materials* 10, 352–356 (2011).
32. F. Roddier, "Interferometric imaging in optical astronomy," *Phys. Reports* 170, 97–166 (1988).
33. P. M. Hinz, J. R. P. Angel, W. F. Hoffmann, D. W. McCarthy, P. C. McGuire, M. Cheselka, J. L. Hora, and N. J. Woolf, "Imaging circumstellar environments with a nulling interferometer," *Nature* 395, 251–253 (1998)

Figure Captions

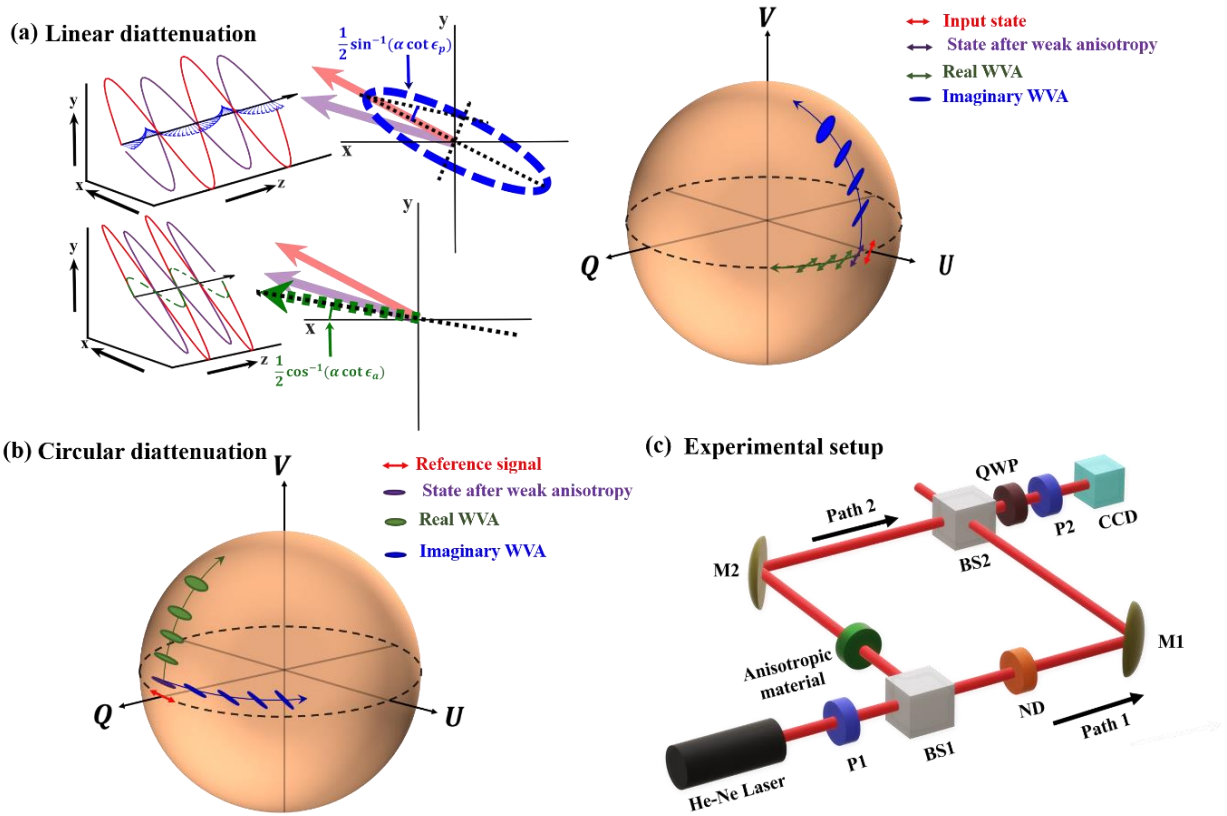


Figure 1: Illustration of the concept of weak value polarimeter. Weak value amplifications of (a) *linear diattenuation* and (b) *circular diattenuation*. (a) A pictorial representation of the electric field vectors and polarization ellipse undergoing imaginary (top left panel) and real (bottom left panel) WVA of *linear diattenuation*. **Top left panel:** The electric fields corresponding to the $+45^\circ$ polarized light in path 1 (red solid line), after experiencing a small linear diattenuation effect in path 2 (violet dotted line) and the resultant field after near destructive interference with small phase offset ϵ_p (blue dashed line). The enhancement of ellipticity as a manifestation of imaginary WVA is also displayed. **Bottom left panel:** The corresponding electric fields for real WVA. The resultant field after near destructive interference with small amplitude offset ϵ_a is shown by green dashed line. The change in the orientation angle of the electric field as a manifestation of real WVA is also displayed. The evolutions of the Stokes vectors in the Poincare sphere for real (green line) and imaginary (blue line) WVA of *linear diattenuation* are shown in the **right** panel. (b) The evolutions of the Stokes vectors in the Poincare sphere for real (green line) and imaginary (blue line) WVA of *circular diattenuation* effect. (c) Schematic of the Mach-Zehnder interferometric arrangement of weak value polarimeter. (P1,P2): polarizers, (BS1, BS2): beam splitters, (M1,M2): mirrors, QWP: quarter waveplate. The weak anisotropy is introduced in path2 using an appropriate polarization optical element.

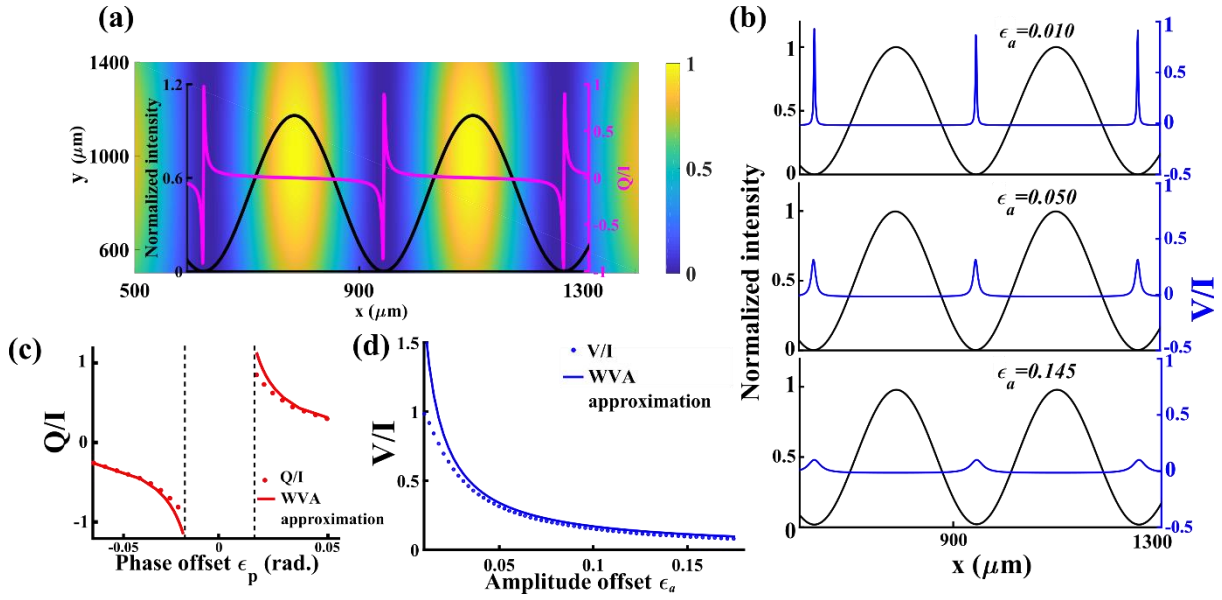


Figure 2: Real and imaginary WVA of linear retardance effect. Simulation of the weak value polarimeter interference experiment (corresponding to set-up Fig. 1c) with small linear retardance as the weak polarization anisotropy effect ($\alpha = 0.017\text{rad}$). **(a)** Typical fringe profile from the interference of $+45^\circ$ polarized Gaussian light beam (beam width = 1mm) in one arm of a Mach-Zehnder interferometer with the beam having a slightly changed polarization state in the other arm. The intensity profile (left axis, black line) and the spatial variation of $\frac{Q}{I}$ Stokes polarization parameter (right axis, red line) along x -axis of the fringe. Here, colour bar represents magnitude of intensity. The $\frac{Q}{I}$ parameter exhibits prominent enhancement around the destructive interference region as a manifestation of *imaginary* WVA. **(b)** The corresponding results for *real* WVA. The intensity profile (left axis, black solid line) and spatial variations of the $\frac{V}{I}$ Stokes parameter (right axis, blue solid line) are shown for three different amplitude offsets $\epsilon_a = 0.010, 0.050, 0.145$. **(c)** The variation of $\frac{Q}{I}$ as a function of the small phase offset ϵ_p (red circles) and theoretical fit to *imaginary* WVA ($\sim \alpha \cot \epsilon_p$) (red line). The region where the WVA approximation breaks down ($\epsilon_p \leq \alpha$) is marked in the figure. **(d)** The variation of $\frac{V}{I}$ as a function of ϵ_a (blue solid circles) and the corresponding *real* WVA fit ($\sim \alpha \cot \epsilon_a$, blue line).

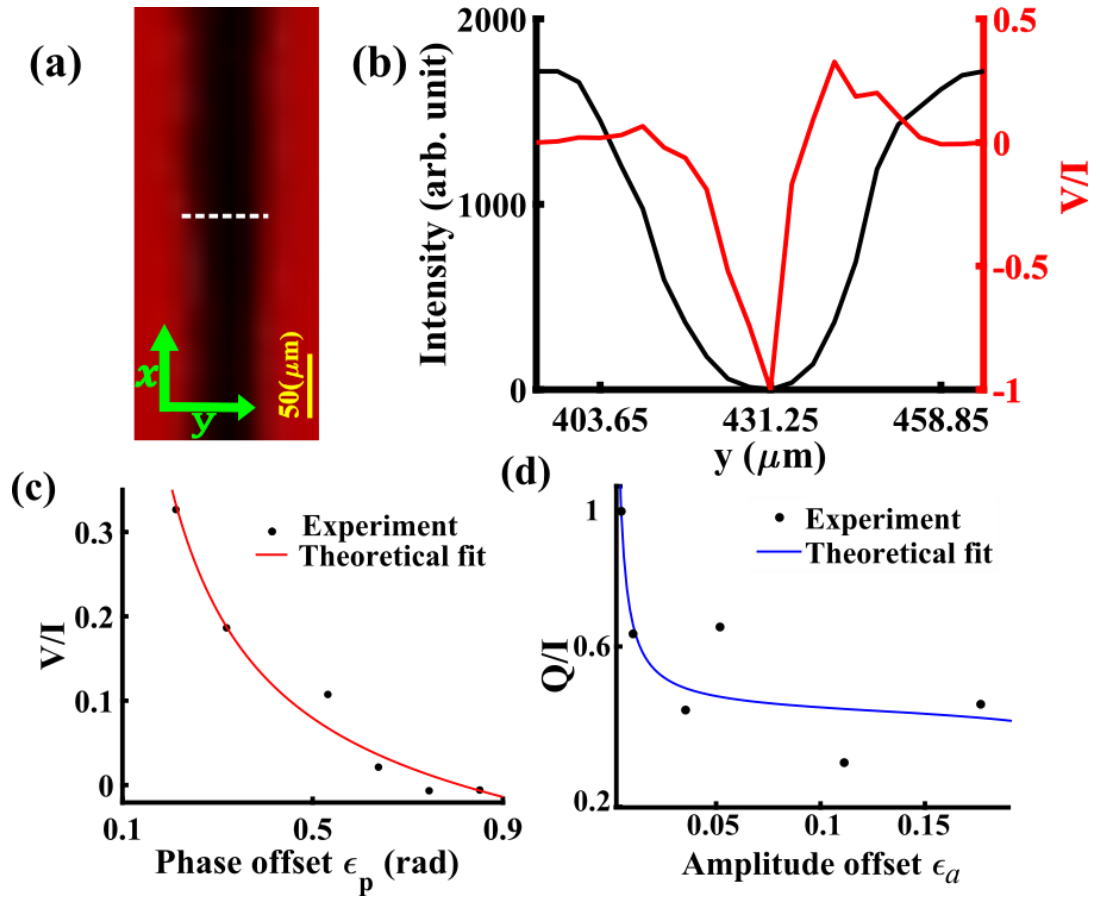


Figure 3: Experimental demonstration of real and imaginary WVA of linear diattenuation effect. Weak linear (x - y) diattenuation (*magnitude* $\alpha = 0.017$) is introduced by placing a linear polarizer at an angle 44° w.r.to the horizontal axis in one arm of the interferometer (Fig. 1c). **(a)** Typical recorded fringe profile shown around the destructive interference point. **(b)** The intensity profile (left axis, black solid line) and spatial variation of $\frac{V}{I}$ Stokes parameter (right axis, red solid line) along the white dashed line marked in (a). Rapid variation of $\frac{V}{I}$ around the position of intensity minima (destructive interference) is a manifestation of *imaginary* WVA. **(c)** The variation of $\frac{V}{I}$ as a function of phase offset ϵ_p (black solid circles) and theoretical fit to *imaginary* WVA ($\alpha \cot \epsilon_p$) (red line). **(d)** The variation of $\frac{Q}{I}$ as a function of ϵ_a (black solid circles) and the corresponding *real* WVA fit ($\alpha \cot \epsilon_a$, blue line).

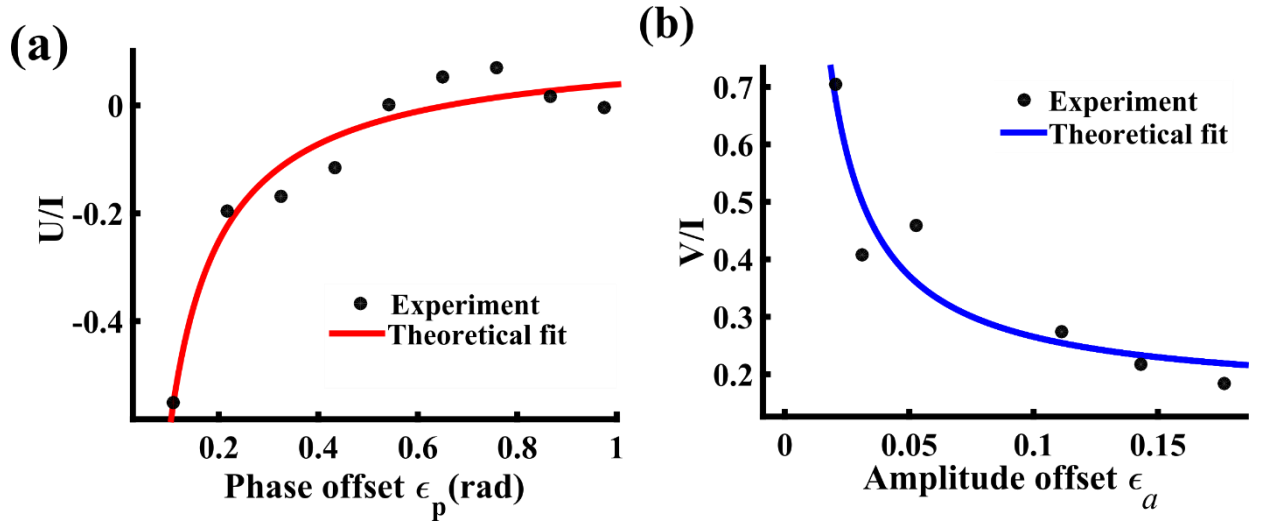


Figure 4: Experimental demonstration of real and imaginary WVA of circular diattenuation effect. Weak circular diattenuation (*magnitude* $\alpha = 0.012$) is introduced in one arm of the interferometer. **(a)** The variation of $\frac{U}{I}$ Stokes parameter as a function of phase offset ϵ_p (circles) and corresponding theoretical fit to *imaginary* WVA ($\alpha \cot \epsilon_p$) (red line). **(b)** The variation of $\frac{V}{I}$ as a function of ϵ_a (black circles) and the corresponding *real* WVA fit ($\alpha \cot \epsilon_a$, blue line). Excellent agreement with the predictions of WVA demonstrates faithful imaginary and real WVA of circular diattenuation effect.

Anisotropy effects	Electric fields		WVA bearing Stokes vector elements		Polarization optical component for experimental realization
	E_1 and input polarization	E_2	Real WVA	Imaginary WVA	
Linear diattenuation ($x - y$)	$\frac{(\hat{x} + \hat{y})}{\sqrt{2}}$ +45° linear	$\frac{e^{\alpha}\hat{x} + e^{-\alpha}\hat{y}}{\sqrt{e^{2\alpha} + e^{-2\alpha}}}$	$\frac{Q}{I}$	$\frac{V}{I}$	Linear polarizer oriented at a small angle from the +45° orientation
Circular diattenuation	$\hat{x} = \frac{(\hat{r} + \hat{t})}{\sqrt{2}}$ Horizontal linear	$\frac{e^{\alpha}\hat{r} + e^{-\alpha}\hat{t}}{\sqrt{e^{2\alpha} + e^{-2\alpha}}}$	$\frac{V}{I}$	$\frac{U}{I}$	Quarter waveplate with its optic axis oriented at a small angle with respect to the horizontal polarization
Linear retardance	$\frac{(\hat{x} + \hat{y})}{\sqrt{2}}$ +45° linear	$\frac{(e^{-i\alpha}\hat{x} + e^{i\alpha}\hat{y})}{\sqrt{2}}$	$\frac{V}{I}$	$\frac{Q}{I}$	Liquid crystal variable retarder with small retardance
Optical rotation	$\hat{x} = \frac{(\hat{r} + \hat{t})}{\sqrt{2}}$ Horizontal linear	$\cos\alpha\hat{x} + \sin\alpha\hat{y}$	$\frac{U}{Q}$	$\frac{V}{I}$	Half waveplate oriented at small angle with respect to the horizontal polarization

Table I: Real and imaginary WVA of all the polarization anisotropy effects. The four different polarization anisotropy effects (1st column), the corresponding input electric field and the electric field after experiencing a small anisotropy effect (2nd column), the Stokes vector elements carrying signature of real and imaginary WVA of respective anisotropy effects (3rd column). The polarization optical components used realize the WVA of respective anisotropy effects are listed in the 4th column.